

Chapter 19

Silk Fibroin Based Technology for Industrial Biomanufacturing



**Valentina Benfenati, Stefano Toffanin, Camilla Chieco, Anna Sagnella,
Nicola Di Virgilio, Tamara Posati, Greta Varchi, Marco Natali,
Giampiero Ruani, Michele Muccini, Federica Rossi and Roberto Zamboni**

Abstract Natural biomaterials are more and more used for the development of high technology solutions, setting the scene for a bio-based material economy that responds to the increasing demand of environmentally friendly products. Among natural biomaterials, silk fibre protein called silk fibroin (SF) produced by the *Bombyx mori* L. insect, recently found a broad range of applications in biomedical field. SF substrates display remarkable properties like controlled biodegradability, flexibility, mechanical resistance and optical transparency, solution processability. These properties combined with the water-based extraction and purification process make SF a promising material for sustainable manufacturing enabling to partially replace synthetic, plastic-based and non-biodegradable material use. The use of SF interfaces in biocompatible electronic or photonic devices for advanced biomedical applications has been recently highlighted. However, the use of a natural biomaterial is challenging due to the complex nature of the biological molecule, and it requires to tightly control biomaterial properties during all the manufacturing steps. In this work, we show the results obtained by in loco production of raw-material, defining the best condition for *silkworm* selection and growth. The assessment and standardization of extraction/purification methodology are reported with reference to the high purity and remarkable performance in terms of chemo-physical property and biocompatibility of the obtained SF products. Finally, we demonstrate the fabrication, characterization and validation of microfluidic and photonic components of a lab-on-a-chip device for biodiagnostic based on biomanufactured SF.

V. Benfenati (✉) · T. Posati · G. Varchi · R. Zamboni
CNR-ISOF, Istituto per la Sintesi Organica e la Fotoreattività, Bologna, Italy
e-mail: valentina.benfenati@isof.cnr.it

S. Toffanin · M. Natali · G. Ruani · M. Muccini
CNR-ISMN, Istituto per lo Studio dei Materiali Nanostrutturati, Bologna, Italy

C. Chieco · N. Di Virgilio · F. Rossi
CNR-IBIMET, Istituto di Biometeorologia, Bologna, Italy

A. Sagnella
Laboratory MIST E-R, Bologna, Italy

© The Author(s) 2019
T. Tolio et al. (eds.), *Factories of the Future*,
https://doi.org/10.1007/978-3-319-94358-9_19

19.1 Scientific and Industrial Motivations

A major challenge toward bio-based economy consists in the replacement of fossil fuels on a broad scale, not only for energy applications, but also for material, clothing and plastic application. In this view, the worldwide trend to a low-carbon economy and sustainable primary production stimulates the use of naturally derived raw materials as alternative resource to oil-based plastics for manufacturing. However, natural materials must be renewable, available, recyclable, and biodegradable to be competitive and they need to be processed by green and sustainable approaches. Moreover, natural biomaterial products should provide a higher technical performance for selected application in comparison to synthetic and plastic based counterpart. In this context, the manufacturing of biomedical devices for diagnostic or therapeutics offers a potential market opportunity for the use of natural biomaterials. Indeed, natural biomaterials due to their well-known intrinsic characteristics such as biodegradability, and high biocompatibility are ideally suited to develop innovative biomedical products such as those for tissue engineering and also medical sensing. Indeed, during the last three decades, the use of natural biomaterials in tissue engineering is rapidly evolving and innovative devices are able to support and recover the structure and the functionalities of injured hosting tissues [1, 2]. Several evidences have consolidated the use of biomacromolecules for development of scaffold devices that enable the regeneration of different tissues (i.e. nerve, cartilage, bone) [1, 2]. Natural biopolymers mainly includes proteins (i.e. collagens, gelatine, zein, silk fibroin, elastin), polysaccharides (i.e. chitin, alginates, chitosan, cellulose derivate), and amides (i.e. starch). Silks are natural proteins polymers produced by different species of insects, such as spiders, scorpions, silkworms [3]. Among silks, Silk fibroin (SF) produced by *Bombyx mori* cocoon have been used clinically as sutures for centuries [3]. Nonetheless, in recent years, SF-based materials have been extensively studied in tissue engineering and drug delivery due to their biocompatibility, slow degradability and remarkable mechanical and optical properties [1–3]. Notably, through a process of reverse engineering Rockwood et al. [4] have defined a water-based and sustainable process that enable to obtain an aqueous-based SF solution, called regenerated silk fibroin (RSF), from the cocoon fibre. The use of the RSF solution is particularly interesting in the context of biomedical application [1–4] because it can be processed in various formats (films, fibres, nets, meshes, membranes, gels, sponges) retaining exceptional chemo-physical and biological properties. In this context, SF displays the potential to be exploited as a raw material to become a technological material platform [3, 5] for eco-sustainable manufacturing. However, some chemical and physical post-processing treatments of SF could damage/denature the protein and completely modifying its primary structure properties, thus altering the properties of the obtained substrates. Nonetheless, when dealing with naturally derived products and biomedical application it is highly desirable to establish and control the whole product lifecycle: from the raw material production to substrate preparation to technology validation. In this view, the goal of our work is to define and control the whole silk chain by in loco production of the raw-material,

the assessment and standardization of extraction/purification methodology the characterization of the chemo-physical and biocompatibility properties of the obtained SF products. Herein, we report on state of the art methods and protocols to use SF as new material for advanced bio-technological application and sustainable manufacturing (Sect. 19.2). The proposed approach is presented in Sect. 19.3 and further detailed in Sect. 19.4, whereas the experiments are reported in Sect. 19.5. In particular, we demonstrate the importance of the definition and control of the whole chain for biomanufacturing underpinning the silk fibroin-based technology. Furthermore, we demonstrate and report the results obtained on the fabrication, characterization and validation of microfluidic and photonic components of a lab-on-a-chip device for biodiagnostic based on biomanufactured SF.

19.2 State of the Art

The progress in material science, biotechnology, photonics and electronics is promising for the development of novel technologies that will dominate the future of health-care and improve the quality of life. Lab-on-a-Chip (LOC) devices have demonstrated to be highly performing for analytical purposes in genetic sequencing, proteomics, and drug discovery applications [6]. However, they are not yet compatible with point-of-care diagnostics applications, where cost and portability are of primary concern. Recent advance in plastic electronics revealed the promising future for oil-based organic (plastic) material for on chip integration of optic, photonic and microfluidic structure to fabricate portable, low-weight and low cost devices. However, global trends towards sustainable development stimulate the use of renewable and biodegradable raw materials and innovative environmental friendly manufacturing of the technology of the future. Naturally occurring (bio-derived) materials provide a compelling template to reinterpret modern manufacturing while rendering it sustainable and green. The challenge to make bio-derived materials a credible alternative to current plastic and synthetic materials and inorganic substrates is to identify materials that, while being environmentally sustainable, display properties that combine chemo-physical, technological end economic need for sustainable biomanufacturing. As an example, the material has to be widely available and cost-competitive within the global supply chain and, at the same time it should maintain adequate chemo-physical and biocompatibility properties to successfully interface with technology intended for biomedical application [1–3, 5]. In this context, natural fibres can provide several benefits such as low cost, *green* origin, abundant and renewable, carbon dioxide neutral, lower densities, recyclability, biodegradability, moderate mechanical properties. Moreover, their mechanical and technological performance shows high potentials in their applications [1–3, 5].

Among natural fibres, SF produced by the silkworm *Bombyx mori* L. has high potentials for a wide range of innovative, green and high-tech applications [3]. Silk fibroin solution, extracted from the cocoon by a water based eco-friendly method [4], could be solution-processed (by spin coating, ink-jet printing, spray draying) in

different forms and substrates with exceptional properties in terms of mechanical flexibility, dielectric properties, biocompatibility, optical transparency and possibility of functionalization with optically/biologically active molecule (drugs, dye, nanoparticles). Thus, silk fibroin offers a unique possibility to enable multiple and complementary approaches for technological and biomedical application.

Among different forms of SF-based biomaterials, SF films can be obtained from regenerated solution RSF with defined thickness (with a range spanning from hundreds nanometers to tens micrometres) by means of liquid processing such as spin coating, inject printing, doctor blade that are suitable for industrial manufacturing. SF films can be also nanostructured by soft lithography, contact printing or nanoimprinting. Nonetheless, silk fibroin can be doped, blended and functionalized to obtain a numerous amount of substrates for advanced technological applications in the biomedical field, such as organic electronic sensors based on field effect transistors [5, 7] for electrophysiological recording of neural cells or optical device such as photonic sensors and optoelectronic devices [8]. In particular, optical and biological properties of silk fibroin films can be enhanced thanks to several processes that are able to functionalize and modify SF with optically active dyes, doping molecules, growth factors and/or chemicals or nanoparticles [9–11]. Among the others, a green and sustainable method to produce innovative modified silk substrates is feeding cocoon with a diet characterised by the addition of doping molecules that enable the biological incorporation of dopant into SF [12–14]. The approach indeed avoids the need of an additional chemical process, and post-treatments associated with it [12–14]. A series of fluorescent dyes have been successfully incorporated in silk fibre by addition of colorant compounds to the mulberry diet [12–14].

The feasibility of using SF materials has been demonstrated *in vitro* and *in vivo* for opto-electronic biomedical applications and for the use in peripheral nerve tissues repair [7, 8, 15–21]. It has been shown that optically transparent, ultrathin and flat silk films can be integrated as dielectric in organic field effect transistor (OFET) and organic light emitting transistor (OLET) architectures [7], also used to stimulate and record cells functional properties [20, 21]. Also, it was demonstrated that silk films can be nano- and micro-patterned to obtain mechanically robust structures with desired optical wavelength size [8]. Organic lasing from a stilbene-doped silk film spin-coated onto a one-dimensional distributed feedback grating (DFB) was demonstrated, with the lasing threshold lower than that of others organic DFB lasers based on the same active dye.

19.3 Problem Statement and Approach

The industrial scale development of silk fibroin based technologies requires the optimization and control of all the silk-fibroin production steps, from the raw material to the technological application. The lack of such control hampers the use of SF at industrial scale and limited the demonstration of silk-based devices at a lab-scale. The aim of our work to establish and control the whole-chain underpinning the fabri-

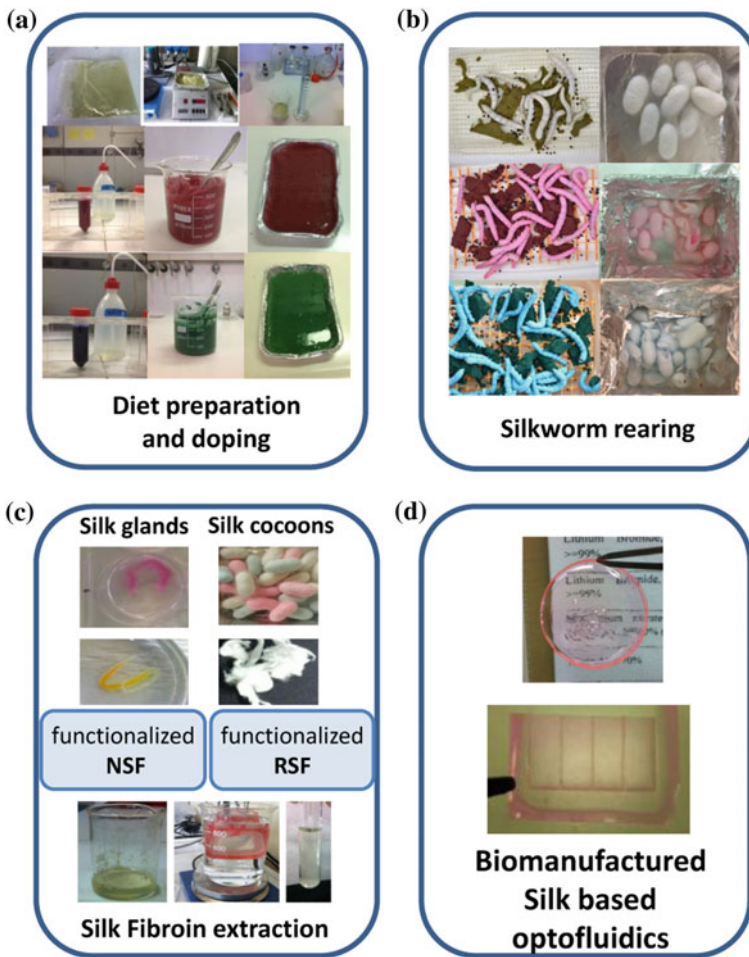


Fig. 19.1 Schematic picture of the biomanufacturing approach to obtain SF based technological substrates

cation of the silk fibroin based technology (Fig. 19.1). The technology of interest is a SF-based innovative lab-on-a-chip (LOC) device for high throughput bio-diagnostic. In particular, the optical based LOC is intended for fluorescence optofluidic detection and sorting of tumour cells.

The design of the proposed biomanufacturing approach consists of the following steps:

- (1) Diet preparation (Fig. 19.1a) and optimization of silkworm breeding (see Fig. 19.1b) to obtain a reproducible, controlled and high quality functionalized silk fibroin. Notably, the production of the raw-material described in this work includes the standardization of a novel process that enables direct func-

tionalization of SF fibres by feeding the cocoon with a diet doped with optically active molecule of interest (Sect. 19.4.1).

- (2) Standardization of the extraction, purification, and characterization of functionalized silk fibroin (native and regenerated) from different races of *B. mori* (see Fig. 19.1c; Sect. 19.4.2).
- (3) Protocols to obtain regenerated silk fibroin (RSF) solutions and then produce RSF films (top of Fig. 19.1d; Sect. 19.4.3).
- (4) Fabrication, characterization and validation of a silk-based photonic and microfluidic component of LOC device (see bottom of Fig. 19.1d; Sect. 19.4.4). Optical and photonics components of the silk based device have been fabricated by using in loco produced and extracted silk fibroin, characterized and validated for the use in optofluidic lab-on-a-chip. Soft lithography and nano-imprinting approaches have been developed for the fabrication. Also, results on AFM topography, optical transparency of the obtained substrate are reported. Biological properties in terms of cell adhesion growth and alignment have been evaluated [22].

19.4 Developed Technologies, Methodologies and Tools

19.4.1 *Protocols for Optimized Silk Production and Fibroin Biodoping*

In order to obtain a reproducible, controlled and high quality functionalized silk fibroin for the production of opto-fluidic devices, optimization of conventional silkworm breeding was performed. By feeding the silkworm larvae with a diet added with a fluorescent dye molecule, Rhodamine B, a biological functionalization of the silk fibroin was promoted. White polyhybrid strains of silkworm coming from germplasm collection of the CRA-API (CRA, Honey bee and Silkworm Research Unit, Padua seat) were reared in plastic boxes (different in size according to the larvae age) placed in a room under controlled conditions (relative humidity >85%; 12:12 L:D photoperiod). During the whole larval stages the insects were fed *ad libitum* with artificial diet provided by CRA-API and prepared avoiding as much as possible the alteration of nutrients contained in it [23].

For protocol definition, the silkworm survival and length of the larval cycle (time between the incubation of the eggs and the cocoons spinning) were monitored at three different breeding temperature conditions ($24\text{ }^{\circ}\text{C} \pm 1$; $26\text{ }^{\circ}\text{C} \pm 1$; $28\text{ }^{\circ}\text{C} \pm 1$). A total number of 185, 408 and 295 larvae were tested at $24\text{ }^{\circ}\text{C} \pm 1$, $26\text{ }^{\circ}\text{C} \pm 1$ and $28\text{ }^{\circ}\text{C} \pm 1$, respectively.

Starting from the 3rd day of the 5th instar, the Rhodamine B has been added to the artificial diet at two different concentrations: 0.05, 0.03 g in 100 g of powder diet. Three groups of ten larvae were used for each concentration against 30 larvae fed with artificial diet without any dyes representing *the blank* control treatment [23].

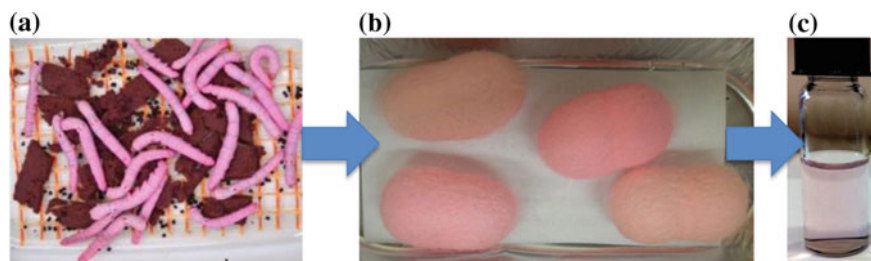


Fig. 19.2 Biomanufacturing of Rhodamine biodoped silk fibroin solution

19.4.2 Protocol for Native Fibroin Extraction

Among different methodologies for fibroin extraction of silk fibroin from *B. mori* cocoon, the reverse engineering methods, developed by Rockwood et al., enable to produce an aqueous regenerated silk fibroin solution, avoiding the use of strong and toxic organic solvent [4]. However, the process is optimized for a lab-scale production and not for extraction of silk containing xenobiotics. The current protocol was modified and optimized to promote up-scaling and to gain the highest concentration of xenobiotic in the silk extracted protein. Methods for extraction of native fibroin from silk glands of a mature 5th instar larvae of silkworm have been reported by Tansil et al. [12, 13]. This method of extraction applied to functionalized silk fibroin cocoons promises to maintain the naturally existing properties of protein and, moreover, allows to investigate the distribution of the dye into silk gland. Suitable revision of the methodology of extraction are reported, that have been carried out in order to optimize and adapt the procedure of protein functionalization and to obtain a high quality fibroin for the production of advanced optical devices (Fig. 19.2).

The whole silk glands were extracted from 5th instar larvae one day before they started to spin. The silkworm was anesthetized by using chloroform. A dorsal incision was carried from the head to sacral side of the larva. After gut removal whole silk glands were pulled out from the abdominal side of the worm. The gland was separated in two parts, the middle part and the posterior part that were treated separately [23].

Two pairs of posterior silk glands (coming from two larvae) was placed into a baker containing 3 ml of distilled water, cut in small pieces, gently shaken for 1 h and then kept in refrigerator overnight. The day after, the protein released into the water by the glandular tissue was collected and stored in refrigerator.

The middle gland was washed in deionized water and individually placed into a glass Petri dish. After the epithelium removal, the proteins were left for 2 h in 3 ml of distilled to dissolve the most soluble sericin. After sericin removal, the remaining protein, was added with 3 ml of distilled water and the solution was kept at ambient temperature for one day until the total dissolution of fibroin. The latter was defined as native silk fibroin solution (NSF).

19.4.3 *Protocols to Obtain Regenerated Silk Fibroin (RSF) Solutions and Films*

The protein extraction was performed testing two different methodologies: the extraction directly from the silkworm silk gland (Native Silk Fibroin, NSF) and the extraction of the protein from silkworm cocoons (Regenerated Silk Fibroin, RSF). The cocoons obtained as described above were processed to obtain RSF, optimizing Rockwood et al., protocol [4]. Cocoon were degummed in boiling 0.02 M Na_2CO_3 (Sigma-Aldrich, St Louis, Mo) solution for 45 min. The SF fibres were then rinsed three times in Milli-Q water and dissolved in a 9.3 M LiBr solution at 60 °C for 6 h. Subsequently, the SF water-solutions were dialyzed (dialysis membranes, MWCO3500) against distilled water for 48 h and centrifuged to obtain pure regenerated SF solutions (ca. 6–7 w/v %). The SF water-solutions were stored at 4 °C [23].

The films were fabricated as follows to characterize chemophysical and biological properties of SF films: a 160 μL aliquot of RSF or Native Silk Fibroin (NSF) dropped on 19 mm diameter glass coverslips and successively dried for 4 h in a sterile hood generating films with a thickness of around 20 μm . A support/mould of polydimethylsiloxane (PDMS) was used as a substrate to obtain free-standing films. The resulting RSF films were used for transmittance test [23].

According to the adopted approach for the realization of a silk-based optofluidic Lab-on-a-Chip device, the microfluidic structures have to accommodate photonic components such as diffraction gratings and optical filters. Thus, the dye-doped regenerated silk fibroin thin-films that are implemented in the micromoulding process have to show the proper characteristics in terms of optical features. In particular, a process protocol was optimized to obtain free-standing fibroin films with the suitable thickness and superficial smoothness in order to guarantee high optical gain and efficient waveguide effect.

A detailed study was performed to fabricate micrometre-thick films of regenerated silk fibroin doped with lasing dye Rhodamine B (RhB) by varying the drop-cast process conditions, substrates (size and material) and post-process thermal treatment. Indeed, it was observed that the drying process of the films has to be performed at 50 °C in a vacuum oven overnight at a pressure ranging from 600 to 800 mbar when using silk fibroin water solution at 5–10% w/v concentration regardless the dye concentration.

Figure 19.3a, b show the images of the film that were obtained from drop-casting RhB-doped regenerated silk fibroin (SF) water-solution at 5% w/v concentration onto high-quality quartz. By preserving the dimensions of the templating substrates ($\sim 4 \text{ cm}^2$), it was possible to control the film thickness by varying the volume of RhB-doped SF solution. Indeed, films of 20 μm (in Fig. 19.3a) and 50 μm (in Fig. 19.3b) thickness were obtained by implementing solution volumes of 0.6 and 1.3 mL, respectively.

Even though it was chosen to use the thicker films with lower dye concentration for the following fabrication steps because of the expected high gain in the optical amplification characterization, it was observed that the glass substrate enables the

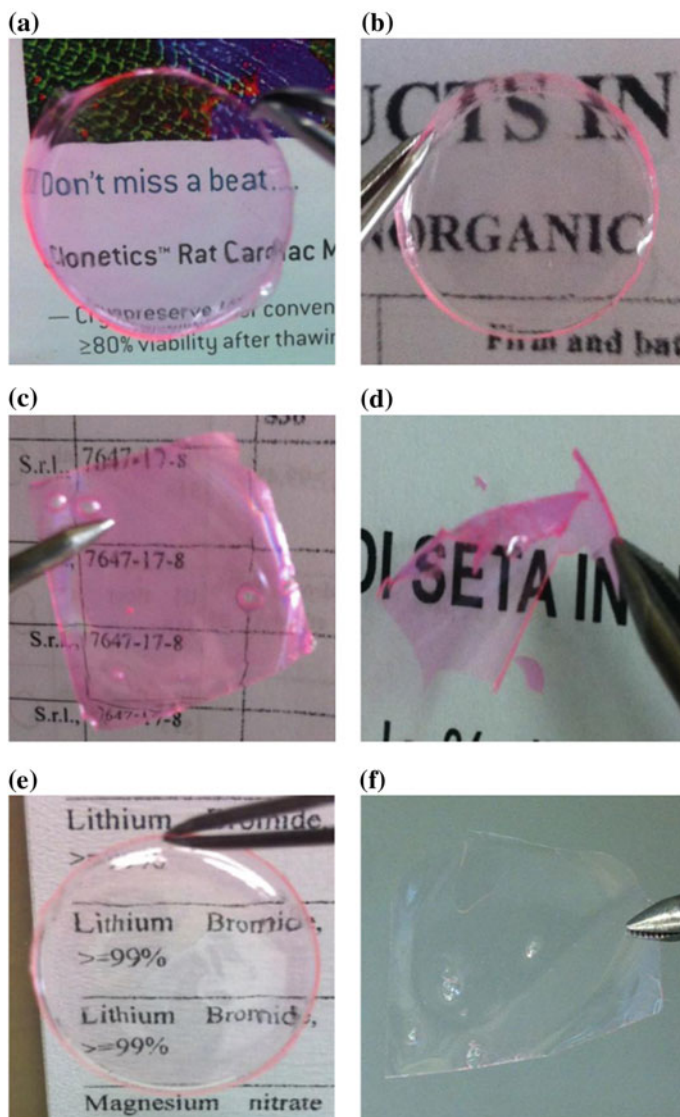


Fig. 19.3 SF films that are obtained by drop-casting a different amount of solution on various substrates and slow drying

realization of homogenous, defect-free and smooth free-standing silk-fibroin films regardless the deposition conditions.

On the other hand, it was observed that the use of different templating substrates did not guarantee the expected quality in silk filmability. Figure 19.3c, d show the images of RhB-doped free standing films obtained by drop-casting 2 mL of SF

water-solution at 5% w/v onto 6 cm²-wide patterned PDMS (Polydimethylsiloxane) (in Fig. 19.3c) and polycarbonate (in Fig. 19.3d) substrates. Indeed, the deposition onto PDMS results into heterogeneous films where millimetre-size air bubbles are clearly visible; the deposition onto polycarbonate results in a very thin film which cracks into pieces due structural rigidity.

Finally, it was demonstrated that the modification of the silkworm diet by artificial doping with dye-laser molecules did not deteriorate the structural properties and processability features of the silk fibroin thin-films. Figure 19.3e, f show that the best performing substrate for drop-casting silk fibroin water-solution is high-quality quartz (in Fig. 19.3e), while the use of PDMS substrate results in fabrication of non-homogeneous and porous thin films as expected (in Fig. 19.3f).

19.4.4 Fabrication of Silk Fibroin Microfluidic Structures

After having optimized the protocol for drop-casting silk fibroin water solutions onto technologically relevant flat substrates with different adhesion properties, a protocol was developed to fabricate microchannels into silk fibroin films for engineering complex microfluidic devices.

The implemented lamination strategy is based on drop-casting silk fibroin water solution to bond replica-moulded water-insoluble silk films. Replica-moulded silk fibroin films cast on PDMS negative moulds could be produced in rapid succession while maintaining a high degree of feature fidelity. Indeed, it is reported in literature that features as small as 400 nm could be produced using this method.

It was demonstrated that the adhesion properties and, thus, the consequent delamination efficiency are strictly dependant on the substrate features. Indeed, unsatisfactory results were obtained by implementing PDMS substrates. Moreover, the accuracy of the replica-moulding technique with patterned substrates is mainly correlated to the specific quality of the substrate surface in terms of roughness and grade of purity. Thus, in collaboration with Laboratory of Industrial Research and Technology Transfer of the High Technology Network of Emilia-Romagna (MISTER), high-quality PDMS patterned substrates were produced. The micromoulds for PDMS were realized using xurography, a rapid prototyping technique for creating microstructures in various films with a cutting plotter. A cutting plotter with a resolution of 100 μm was used. This technique has the advantage of being inexpensive and permits rapid prototyping of microfluidic devices. This microfabrication technique uses the cutting plotter to directly create microstructures in vinyl films, without photolithographic processes or chemicals. Then, positive and negative microstructures in vinyl films were fabricated, with channels width ranging from 150 to 250 μm . After cutting, unnecessary parts are peeled off the release liner. An application tape is used to hold structures in place while transferring into a petri dish. PDMS was moulded on positive and negative microstructures cut in vinyl. PDMS pre-polymer was mixed with a curing agent (SYLGARD 184, Dow Corning) at a 5:1 weight ratio and then poured into the petri dish. The PDMS mixture was degassed to remove

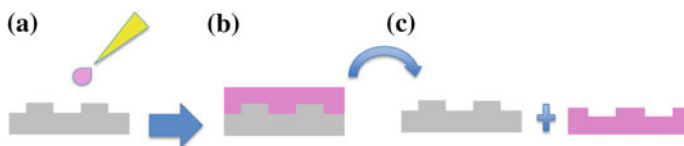


Fig. 19.4 Fabrication procedure for silk fibroin microfluidic channels: **a** drop casting of SF on micropatterned PDMS mould, **b** slow drying and film self-assembly, **c** peal-off of micropatterned silk film

air bubbles and cured at 70 °C. The cured PDMS was then peeled away from the moulds. Finally, micro-patterns were realized on the dye-doped films of silk fibroin according to the process flow that is sketches in Fig. 19.4.

Samples were fabricated from dye-doped and blank regenerated silk fibroin water solutions at 5% w/v. The previously-optimized deposition protocol was implemented in order to obtain films with approximately 100 microns in thickness by controlling the volume to surface area ratio during casting.

Silk solutions were cast on both micromoulded PDMS negative moulds and flat PDMS substrates through water evaporation that was obtained by introducing the films in a vacuum oven overnight at temperature of 50 °C and pressure which is regulated in the range between 600–800 mbar. In this way it is possible to produce water-stable films, which are easily delaminated without any treatments. Differently from what previously reported in literature, it was not necessary to use any solutions for modifying the hydrosolubility of silk-fibroin films or for increasing the delamination efficiency.

Figure 19.5 shows the images of the micromoulded RhB-doped and blank films of silk fibroin after delamination. As it is evident, the fidelity in the reproduction of the features of the negative moulds is very high onto cm²-wide area. Though, further improvements in the procedure have to be achieved in order to avoid the trapping of water bubbles in the films during the evaporation in the oven.

The dye-doped microfluidic device has been characterized in order to verify if the photonic properties of the blend are preserved in channel regions where the optical stimulation and detection are located in the final optofluidic Lab-on-a-Chip.

The silk microfluidic devices were further characterized by performing imaging onto moulded microchannels by implementing optical microscopy in transmission mode in the case of the white silk fibroin sample so that the signal collected is the photoluminescence of the RhB dye molecules dispersed in the silk fibroin film (Fig. 19.5e–f).

The geometrical features of the negative mould are preserved in the laminated films. In fact, a channel width of 70 μm was measured as expected. The walls of the channels are sharply defined for all the samples fabricated even though some material removed from the channel is still deposited onto the wall borders (darker areas in Fig. 19.5e).

Therefore, it was possible to engineer and optimize: (i) a drop-cast deposition technique for obtaining optically high-quality, water-insoluble and free-standing dye-

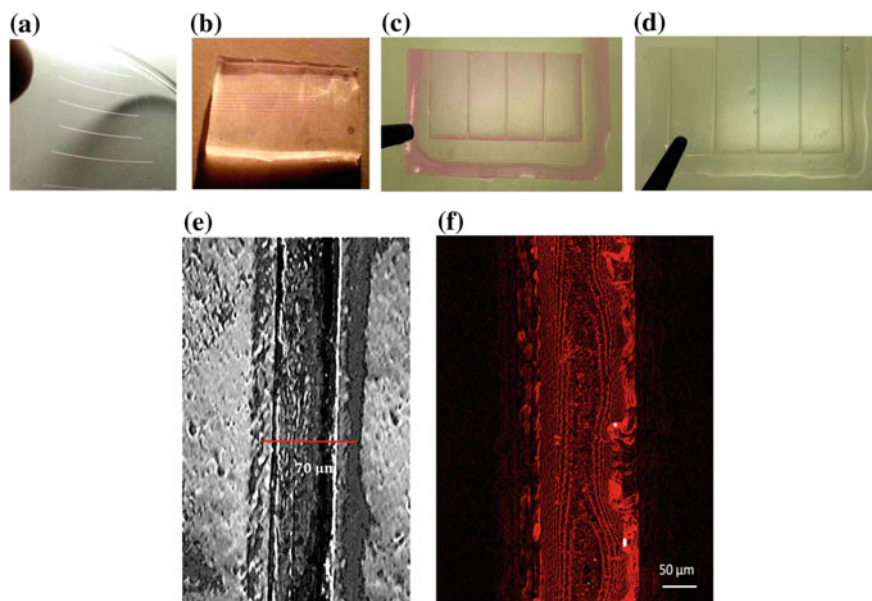


Fig. 19.5 Images of the negative moulds in PDMS. Images of the micromoulded silk fibroin films obtained from RhB-doped (c) and white (d) silk fibroin water solutions. **e** Optical microphotograph of the channel moulded into the blank (reference) sample. **f** Confocal Laser Scanning Microscope image of the channel moulded into the RhB-doped sample

doped silk fibroin films and (ii) a device component fabrication approach capable for the rapid and scalable production of silk-fibroin-based microfluidic devices for cell-seeding without the need for harsh processing conditions or cytotoxic compounds. The techniques employed in this experimental approach are scalable by designing systems with increased surface area and lamination of multiple layers.

19.5 Testing and Validation

19.5.1 Validation of Protocols for Fibroin Production and Functionalization

The first step of our study was to optimize the protocols to rear the *B. mori* worm for the production of raw material for high technological purposes (see Sect. 19.4.1). In particular, each step of breeding was monitored and the best breeding condition were selected [23]. Among different parameters monitored (humidity, temperature, amount of feed, light/dark exposure), we verified that temperature is the most important parameter to be controlled for successful and high yield breeding. In particular,

Table 19.1 Data on larval mortality (%) and on duration of the larval stage (gg)

| Temperature (°C) | Mortality (%) | Mortality in 5th instar (%) | Length cycle (gg) |
|------------------|---------------|-----------------------------|-------------------|
| 24 | 29.3 | 0 | 45 |
| 26 | 13.2 | 0 | 35 |
| 28 | 69.6 | 34.9 | 32 |

Table 19.2 Data on mortality in 5th instar larvae feed with diet added with different Rhodamine B concentration

| Concentration (%) | Mortality in 5th instar (%) |
|-------------------|-----------------------------|
| 0.03 | 3.33 |
| 0.05 | 30 |

our results demonstrated that the optimal temperature for *B. mori* L. breeding is $26\text{ }^{\circ}\text{C} \pm 1$ [23]. From the experiments carried out, it resulted that the higher larval survival percentage was indeed at $26\text{ }^{\circ}\text{C}$. With temperature of $28\text{ }^{\circ}\text{C}$ the percentage of dead resulted almost of 70%, with a 34% of dead occurring during the 5th instar. At $28\text{ }^{\circ}\text{C}$ the duration of the larval cycle was minimum, while at $24\text{ }^{\circ}\text{C}$ cycle duration was too long to be acceptable (Table 19.1). These data demonstrate that length cycle was correlated with the temperature of breeding.

Our results suggested that $26\text{ }^{\circ}\text{C} \pm 1$, even if determinate a little longer larval cycle duration respect to $28\text{ }^{\circ}\text{C}$, is an optimal temperature for an efficient and scalable silkworm breeding.

The results about the association between the larvae mortality and the concentration of the Rhodamine B are shown in Table 19.2.

The dye was administrated to the larvae only during the last larval instar (5th), when the greatest synthesis of fibroin and sericin into the silk glands occurs. Administrated at 0.05% Rhodamine B caused a mortality of 30% in larvae of 5th instar. An acceptable percentage of dead (3.3%) was recorded using lower dye concentration. So, the protocol for production of biologically functionalized fibroin with Rhodamine B has been set up at the concentration of 0.03%.

19.5.1.1 Chemo-Physical Properties of Regenerated and Native Silk Fibroin Solution and Film Obtained from SILK.IT Fab

Chemo-physical properties of Regenerated and Native Silk Fibroin solution and film obtained from in loco produced raw material (*B. mori* cocoon) were analysed. Nuclear Magnetic Resonance (NMR) and FourierTransformed-InfraRed spectroscopy (FT-IR) have been performed to define the composition and the conformational structure of silk fibroin extracted from RSF and NSF.

In particular, the ^1H NMR spectrum of RSF in deuterated water (Fig. 19.6a), recorded at room temperature, confirmed that the sample obtained by our procedure

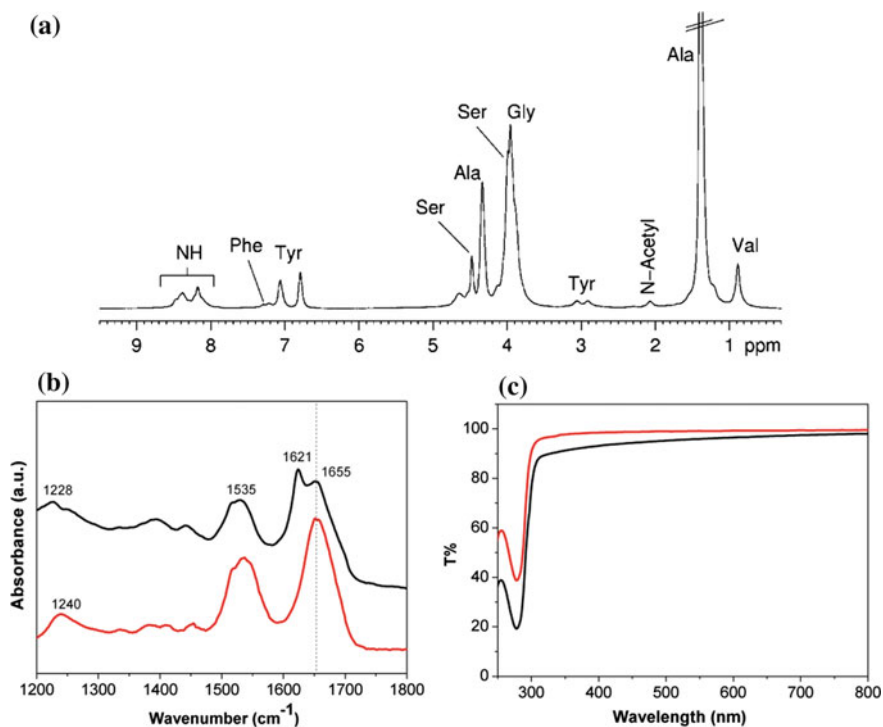


Fig. 19.6 Chemo-physical properties of in loco produced RSF and NSF solution and films [23]

is pure and that the aminoacids composition is in accordance with previous literature report [23, 24].

SF conformation influences the biodegradation, mechanical and optical properties of the SF films. In particular, it is known that a conformational structure with dominance of random coils and alpha-helices (called silk I structure) is highly water soluble and highly biodegradable with respects to the silk II structure, characterized by elevated presence of secondary structures and crystalline formats such as β -sheet.

In order to get further insight on the conformational structure of SF protein in SF films obtained from NSF and RSF, we performed comparative analyses of FT-IR spectra on films prepared from NSF and RSF (Fig. 19.6b). The results reported in Fig. 19.6, revealed that NSF, together with the bands assigned to silk I conformation, display peaks generally attributed to silk II structure. These results indicated that a β -sheet structure is present in NSF (Fig. 19.6b). In this view, it is expected that the biodegradability of NSF is slower than the one of RSF, and that optical properties can be modified. Accordingly, analyses of transmittance of regenerated and native SF films in the UV-visible range, revealed that the regenerated SF film is transparent in the visible region (300–800 nm). Silk fibroin Aromatic aminoacid Tyrosine (Tyr) and Tryptophan absorbance at 274–277 nm account for the decrease observed at the

corresponding wavelength. The transparency of native SF within the same region was 70–90%, thus lower than regenerated SF film (Fig. 19.6c).

19.5.1.2 Properties of Biodoped Silk Films

We next demonstrated that the cocoons of *Bombyx mori* fed with a Rhodamine B (RhB) added diet were coloured and enabled the extraction and purification of RSF and SF films containing RhB [13]. Films were optically transparent and fluorescent with UV-Vis properties typical of RhodamineB added to white natural RSF. Comparative analyses of optical and vibrational features of RhB biodoped SF solution and films with those of white SF blended with RhB were performed, revealing significant difference, suggesting that silkworms' metabolism could be involved in binding mechanism of SF with RhB (for details see [14]).

19.5.1.3 Biological Properties of Silk Films Prepared by Different Methods

The control of the chemo-physical properties of SF films plays a key role in the preparation of tailored SF-based biomaterials and composites targeting optoelectronic devices and photonics technologies intended for biomedical applications such as cell phenotyping. We have then demonstrated that the application of different fabrication methods to prepare SF films influences the chemo-physical properties of SF films and their interaction with neural cells. In particular, we found that hydrophobic surfaces induce proliferation of astrocytes and neuron adhesion, whereas hydrophilic surfaces promote a remarkable neurite outgrowth [24].

Interestingly, surface properties such as roughness and wettability, mechanical resistance, dissolution and degradation profiles can be affected by fabrication method. These properties drive the interaction of SF films with primary neural cells, namely astrocytes and neurons [24]. Also we studied the effect of micro and nanopatterning on cell growth. Notably, micropatterned silk films promoted strong alignment of primary astrocytes with a high dependence from the groove depth and width (Fig. 19.7).

19.5.1.4 Integration of Silk-Based Photonic Structures into Microfluidic Devices and Validation

We aim at estimating quantitatively the amount of laser dye molecules present in the silk fibroin thin-films naturally functionalized with Rhodamine B (RhB), which is necessary for allowing optical amplification process. As we have already discussed in the previous section, we succeeded in demonstrating the feasibility of the process of directly feeding larvae of *B. mori* with specific dye molecules in order to achieve optically active silk fibroin substrates.

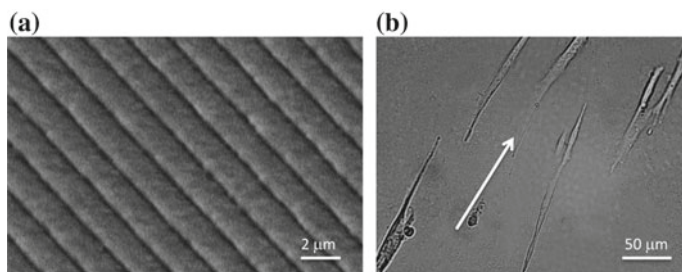


Fig. 19.7 **a** SEM image of micropatterned SF substrate. **b** Micrograph of astrocytes aligned on the substrate of silk micropatterned substrate

After having discriminated which is the most efficient protocol for doping silk fibroin substrates, we demonstrated the maintenance of the photonic features of the most performing dye-doped silk fibroin substrate once structured into a microfluidic device.

We report on the amplified stimulated emission (ASE) characterization performed on silk-fibrin films obtained from blending the regenerated silk fibroin water-solutions at 5% w/v with RhB at different concentrations (i.e. 10^{-6} , 5×10^{-6} , 10^{-5} M): we compared the extrapolated figures of merit with the ones obtained by characterizing the naturally-doped silk fibroin substrates. By means of this comparison we are able to estimate empirically the amount of RhB dye molecules in naturally-doped samples. The ASE characterization was carried out as follows. The samples were measured under vacuum to prevent photo-degradation upon irradiation. The laser beam of a Q-switched Nd:Yag laser was focused onto the sample using a cylindrical lens in order to obtain a rectangular stripe of about $100 \mu\text{m}$ width. The light excitation was the 532 nm frequency-doubled line of the laser with temporal pulse width of 4 ns and 10 Hz of repetition rate. The ASE signal is collected in fibre at 90° with respect the impinging laser by using an optical multichannel analyser. The samples were cut into strips of 4 mm width and about 10 mm length. Moreover, the DIO Board was set to generate the trigger signal to start the spectral acquisition once the excitation pulse was delivered. Thus, the ASE signal is excited by laser single-shot and collected in an automated mode, thus avoiding any possible degradation of the sample.

Figure 19.8 shows the curves displaying the functional dependence from energy per pulse of the full-width-at-the-half maximum (FWHM) values of the RhB emission peak for the three different doped silk-based films. In particular, a silk fibroin film doped at 10^{-5} M with RhB (a), a RhB naturally-doped silk fibroin film obtained from regenerating white polyhybrid strain silkworm (b) and RhB naturally-doped silk fibroin films obtained from regenerating Nistari silkworm (c). In the case of the 10^{-5} M RhB doped silk fibroin film the expected threshold-like behaviour is evident with an abrupt onset of the ASE process at around $70 \mu\text{J}/\text{pulse}$.

Indeed, we performed the ASE characterization protocol on different doped silk fibroin films by varying the dopant concentration (after having verified that the film

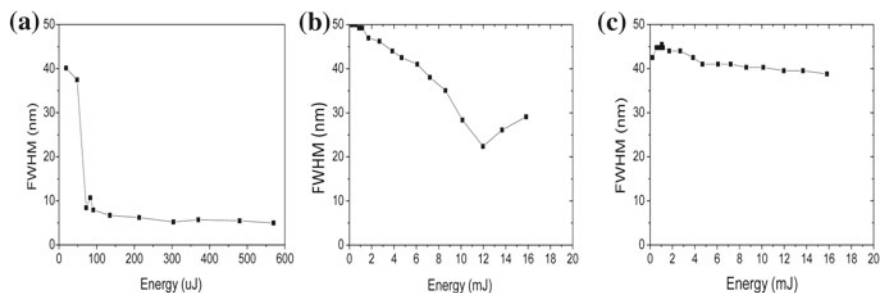


Fig. 19.8 Full-Width-at-the-Half-Maximum (right) *versus* the impinging energy per pulse graphs in the case of **a** silk fibroin sample doped at 10^{-5} M with RhB **b** RhB naturally-doped silk fibroin films obtained from regenerating white polyhybrid strain silkworm and **c** RhB naturally-doped silk fibroin films obtained from regenerating Nistari silkworm

Table 19.3 ASE threshold values in doped silk fibroin films as a function of the RhB dye concentration

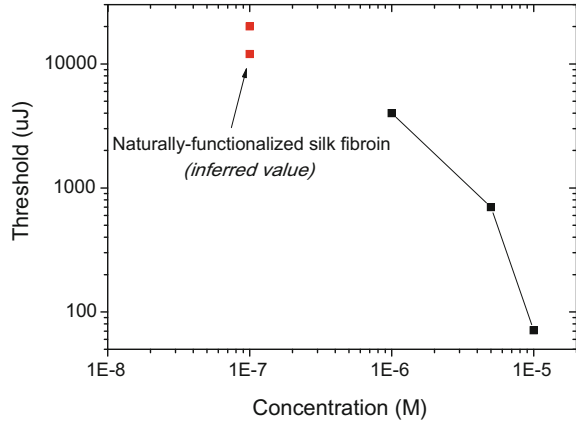
| Concentration M | Threshold energy (μ J) | FWHM (nm) |
|--------------------|-----------------------------|-----------|
| 10^{-6} | >4000 | 16 |
| 5×10^{-6} | 700 | 7.5 |
| 10^{-5} | 71 | 5.5 |

thickness for the different samples is comparable). In Table 19.3 we report the ASE threshold values we estimated as a function of the RhB dye concentration.

We have to mention that in the case of the 10^{-6} M sample a clear threshold of ASE process cannot be identified, given that the FWHM decreases from an initial 45 nm value to about 15 nm almost linearly as the input energy/pulse increases. On the other hand, for samples with concentration at 5×10^{-6} M the beginning of amplification process is observed for energies above 700 μ J. Also in this case, the onset is not abrupt and the samples tend to degrade quickly upon further measurements. Then we compared the ASE threshold values of the blended films with ones of the naturally functionalized films. In particular, we implemented the regenerated silk fibroin solution extracted from the silkworm of two different races: the standard worm (white polyhybrid strain) and the Nistari race.

Figure 19.8b, c show the curves of FWHM as a function of the input energy/per pulse for the standard-worm and the Nistari naturally-doped silk fibroin thin-films, respectively. As it can be observed, no ASE threshold is achieved even at the highest possible fluences with the available laser pump; only in the case of regenerated silk fibroin obtained from the standard-race silkworm an incipient peak narrowing up to 30 nm is detectable before the sample is severely damaged. This result suggests that the amount of Rhodamine B molecules present in the naturally-functionalized silk fibroin films is at least less than 10^{-6} M, possibly as low as 10^{-7} M from the empirical estimation reported in Fig. 19.9.

Fig. 19.9 Estimation of the RhB dye concentration in naturally-functionalized silk fibroin inferred from the measured ASE threshold trend (red squares in the graph)



From these results, considered that a minimum concentration of about 5×10^{-6} M is necessary for the blended sample to be operated in population inversion, we can infer that the naturally-functionalized silk fibroin substrates cannot be efficiently implemented as gain material in biocompatible nanostructured organic lasers. Thus, we implemented RhB-doped silk fibroin substrate obtained from blending regenerated silk fibroin water solution with RhB water solution at 10^{-5} M in the micro-moulded fabrication protocol for achieving microfluidic devices. Indeed, in the Lab-on-a-Chip (LOC) scheme that we propose the microfluidic device component is endowed with the optimized photonic structure for allowing higher degree of miniaturization. For this purpose, we decided to implement in the fabrication of the LOC the best performing silk fibroin substrate in terms of photonic characteristics.

As a final validation of the entire fabrication protocol, we checked the preservation of the photonic characteristics of the RhB-doped silk fibroin material in the channel region of the microfluidic device. Indeed, by using a $100 \mu\text{m}$ -width laser spot it is assured to probe only the region where the micromoulding is present.

As expected, we observed that the efficiency of ASE process is preserved in the channels of the microfluidic device as it is evidenced by the maintenance of the threshold values with respect to unmoulded samples (data not reported), regardless the location of the channels in the device. Only a variation in the maximum achievable output intensity is observed from region to region but this spot-location dependence is expected within the fabricated devices variability. Thus, we can conclude that the micromoulding process that we engineered did not increase the photon losses or degrade waveguiding properties inherent to the optimized RhB-doped silk fibroin substrate.

19.6 Conclusions and Future Research

In this work we addressed the assessment of whole chain production and validation of SF-based substrates and technology for biomedical applications. Our goal was to standardize and optimize methods and protocols to use this silk fibroin as new material for advanced bio-technological application and sustainable manufacturing.

A protocol was developed for fibroin cocoon breeding and feeding for functionalization via bio-doping [23]. The biological incorporation of doping dye molecules into SF by means of feeding cocoon avoid the need for an external chemical process associated with the use of toxic solvents, thus it is an eco-friendly and innovative method to produce doped silk substrates. Tansil et al. [12, 13] demonstrated the ability to include several xenobiotics in the silk fibre by feeding the cocoon with diet modified by addition of selected molecule. We reported results showing the effect of xenobiotic addition to the diet on the larval survival as well as on modification and optimization of breeding conditions [23].

Protocols were defined for the extraction, purification and chemophysical characterization of regenerated fibroin from standard and biodoped cocoon [14, 25]. In this work we saw that adequate extraction and preparation of the RSF and NSF solution coming from the diet doped cocoon results in colour solutions and films [14, 25]. The incorporation by doping and blending of organic dyes in water based silk fibroin [26] might be problematic due to lipophilic nature of the majority of these high quantum yield optically active molecules. In this view, analyses and comparison of samples obtained by blending and addition to SF solution of the selected compound with samples obtained by doping diet method revealed that the sample obtained by doping diet method displays a similar efficiency of functionalization of the substrates. Moreover the method does not affect SF structural, chemophysical and biological property [14, 24, 27, 28].

We have previously shown that DFB and multilayer photonic crystal can be fabricated by silk fibroin doping with stilbene. Herein, we have shown that the same structure can be obtained by using doped and biodoped silk fibroin obtained by in loco produced, extracted and purified raw material. Also soft lithography procedures can be applied to biodoped SF film, to obtain microfluidic chip [25, 29, 30] and this opens the view for industrial scale up of biomanufacturing of SF.

An important issue when dealing with biomedical applications is achieving a true biocompatibility. In this view, we have reported here that plating neural cells, called astrocytes, on micro-nanostructured SF enables their alignment and growth. For biomedical application targeting direct interaction of biological samples with the biomaterials, it is fundamental to study and to understand the effect of chemophysical properties of the biomaterial on cell adhesion, growth, differentiation and behaviour [24]. To reach the goal of integrating SF in a LOC optofluidic device for single cell analyses, it was fundamental to observe if the analysed astroglial cell could be driven to a specific position by following the patterned structure. The feasibility of the proposed approach indicated by the observation reported in Fig. 19.7, complete

the picture to validate the use of nanopatterned SF, fabricated in loco with controlled condition in advanced technological device for cell biosensing.

Studies to integrate optofluidic component in one LOC for diagnosis of brain pathologies such brain tumours are under investigation. Moreover, we are exploring the possibility of exploitation of a direct application in biomaterials and biomedical field of coloured silk fibroin extracted from coloured cocoons [31, 32]. The results reported here were the basis for application for national, private sector supported projects, for the development of silk-based anti-counterfeiting technologies and for European initiatives regarding biomedical use of silk fibroin.

Acknowledgements This work has been funded by the Italian Ministry of Education, Universities and Research (MIUR) under the Flagship Project “Factories of the Future—Italy” (Progetto Bandiera “La Fabbrica del Futuro”) [33], Sottoprogetto 1, research projects “SILK Italian Technology for industrial biomanufacturing” (SILK.IT).

Assunta Pistone, Susanna Cavallini, Giovanni Donati, Simone Bonetti are acknowledged for the work provided within the project. Simone Sugliani from Laboratory MIST E-R is acknowledged for the support on microfluidics fabrication. Marco Caprini and Alessia Minardi from FABIT Dept. of the University of Bologna are acknowledged for the support in the preparation and maintenance of cell culture according to approved Ethical protocol from Italian Ministry of Health (360/2017-PR, approved 05/2017).

References

1. Guarino V, Benfenati V, Cruz Maya IM, Saracino E, Zamboni R, Ambrosio L (2018) Natural proteins for 3D scaffolds in tissue engineering. book chapter. In: Elsevier Press. <https://doi.org/10.1016/b978-0-08-100979-6.00002-1>
2. Guarino V, Benfenati V, Cruz Maya I, Borrachero-Conejo AI, Zamboni R, Ambrosio L (2018) Bioinspired scaffolds for bone and neural tissue engineering. book chapter. In: Elsevier Press. <https://doi.org/10.1016/b978-0-08-100979-6.00003-3>
3. Tao H, Kaplan DL, Omenetto FG (2012) Silk materials—a road to sustainable high technology. *Adv Mater* 24:2824–2837
4. Rockwood DN, Preda RC, Yücel T, Wang X, Lovett ML, Kaplan DL (2011) Materials fabrication from *Bombyx mori* silk fibroin. *Nat Protoc* 6:1612
5. Bettinger C, Bao Z (2010) Biomaterials-Based Organic Electronic. *Polym Int* 59(5):563–567
6. Webb AB, Chimenti M, Jacobson MP, Barber DL (2011) Dysregulated pH: a perfect storm for cancer progression. *Nat Rev Cancer* 11(9):671–677
7. Capelli R, Amsden JJ, Generali G, Toffanin S, Benfenati V, Muccini M, Kaplan DL, Omenetto FG, Zamboni R (2011) Integration of silk protein in organic and light-emitting transistors. *Org Electron* 12(7):1146–1151
8. Toffanin S, Kim S, Cavallini S, Natali M, Benfenati V, Amsden JJ, Kaplan DL, Zamboni R, Muccini M, Omenetto FG (2012) Low-threshold blue lasing from silk fibroin thin films. *Appl Phys Lett* 101:091110
9. Kim DH, Kim YS, Amsden J, Panilaitis B, Kaplan DL, Omenetto FG (2009) Silicon electronics on silk as a path to bioresorbable, implantable devices. *Appl Phys Lett* 95(13):133701
10. Kim DH, Viventi J, Amsden JJ, Xiao J, Vigeland L, Kim YS, Blanco JA, Panilaitis B, Frechette ES, Contreras D, Kaplan DL, Omenetto FG, Huang Y, Hwang KC, Zakin MR, Litt B, Rogers JA (2010) Dissolvable films of silk fibroin for ultrathin conformal bio-integrated electronics. *Nat Mater* 9(6):511–517

11. Melucci M, Zamboni R (2015) Organic materials—silk fibroin synergies: a chemical point of view In: Andrews DL, Grote JG (eds) *New horizons in nanoscience and engineering*. SPIE Press Book
12. Tansil NC, Li Y, Teng CP, Zhang S, Win KY, Chen X, Liu XY, Han MY (2011) Intrinsically colored and luminescent silk. *Adv Mater* 23(12):1463–1466
13. Tansil NC, Koh LD, Han MY (2012) Functional silk: colored and luminescent. *Adv Mater* 24(11):1388–1397
14. Sagnella A, Chieco C, Di Virgilio N, Toffanin S, Posati T, Pistone A, Bonetti S, Muccini M, Ruani G, Benfenati V, Rossi F, Zamboni R (2014) Bio-doping of regenerated silk fibroin solution and films: a green route for biomanufacturing. *RSC Adv* 4:33687–33694
15. Altman GH, Diaz F, Jakuba C, Calabro T, Horan RL, Chen J, Lu H, Richmond J, Kaplan DL (2003) Silk-based biomaterials. *Biomaterials* 24:401
16. Yang Y, Ding F, Wu J, Hu W, Liu W, Liu J, Gu X (2007) Development and evaluation of silk fibroin-based nerve grafts used for peripheral nerve regeneration. *Biomaterials* 28:5526
17. Madduri S, Papaloizos M, Gander B (2010) Trophically and topographically functionalized silk fibroin nerve conduits for guided peripheral nerve regeneration. *Biomaterials* 31(8):2323
18. Benfenati V, Toffanin S, Capelli R, Camassa LM, Ferroni S, Kaplan DL, Omenetto FG, Muccini M, Zamboni R (2010) A silk platform that enables electrophysiology and targeted drug delivery in brain astroglial cells. *Biomaterials* 31:7883–7891
19. Benfenati V, Stahl K, Gomis-Perez C, Toffanin S, Sagnella A, Torp R, Kaplan DL, Ruani G, Omenetto FG, Zamboni R, Muccini M (2012) Biofunctional silk/neuron interfaces. *Adv Fun Mater* 22:1871
20. Benfenati V, Toffanin S, Bonetti S, Turatti G, Pistone A, Chiappalone M, Sagnella A, Stefani A, Generali G, Ruani G, Saguatti D, Zamboni R, Muccini M (2013) A transparent organic transistor for bidirectional stimulation and recording of primary neurons. *Nat Mater* 12:672–677
21. Toffanin S, Benfenati V, Pistone A, Bonetti S, Koopman W, Posati T, Sagnella A, Natali M, Zamboni R, Ruani G, Muccini M (2013) N-type perylene-based organic semiconductors for functional neural interfacing. *J Mater Chem B* 1(31):3850
22. Tung YC, Huang NT, Oh BR, Patra B, Pan CC, Qiu T, Chu PK, Zhang W, Kurabayashi K (2012) Optofluidic detection for cellular phenotyping. *Lab Chip* 12:3552–3565
23. Sagnella A, Chieco C, Di Virgilio N, Toffanin S, Cavallini S, Posati T, Pistone A, Varchi G, Muccini M, Ruani G, Benfenati V, Zamboni R, Rossi F (2015) Silk.it project: Silk italian technology for industrial biomanufacturing. *J Composite B* 281–287
24. Sagnella A, Pistone A, Bonetti S, Donnadio A, Saracino E, Nocchetti M, Dionigi C, Ruani G, Muccini M, Posati T, Benfenati V, Zamboni R (2016) Effect of different fabrication methods on the chemo-physical properties of silk fibroin films and on their interaction with neural cells. *RSC Adv* 11:9304–9314
25. Cavallini S, Toffanin S, Chieco C, Sagnella A, Formaggio F, Pistone A, Posati T, Natali M, Caprini M, Benfenati V, Di Virgilio N, Ruani G, Muccini M, Zamboni R, Rossi F (2015) Naturally functionalized silk as useful material for photonic applications. *J Composite Part B* 71:152–158
26. Posati T, Melucci M, Benfenati V, Durso V, Nocchetti M, Cavallini S, Toffanin S, Sagnella A, Pistone A, Muccini M, Ruani G, Zamboni R (2014) Selective MW-assisted surface chemical tailoring of hydrocalcites for fluorescent and biocompatible nanocomposites. *RSC Adv* 4:11840–11847
27. Sagnella A, Zamboni M, Durso M, Posati T, Del Rio A, Donnadio A, Mazzanti A, Pistone A, Ruani G, Zamboni R, Benfenati V, Melucci M (2015) APTES mediated modular modification of regenerated silk fibroin in a water solution. *RSC Adv* 5:63401–63406
28. Posati T, Benfenati V, Sagnella A, Pistone A, Nocchetti M, Donnadio A, Ruani G, Zamboni R, Muccini M (2014) Innovative multifunctional silk fibroin and hydrocalcite nanocomposites: a synergic effect of the components. *Biomacromol* 15:158–168
29. Prosa M, Sagnella A, Posati T, Tessarolo M, Bolognesi M, Posati T, Toffanin S, Cavallini S, Benfenati V, Seri M, Ruani G, Muccini M, Zamboni R (2014) Integration of a silk fibroin based film as luminescent down-shifting layer in ITO-free organic solar cells. *RSC Adv* 84:44815–44822

30. Benfenati V, Martino N, Antognazza MR, Pistone A, Toffanin S, Ferroni S, Lanzani G, Muccini M (2014) Photostimulation of whole-cell conductance in primary rat neocortical astrocytes mediated by organic semiconducting thin films. *Adv Healthc Mater* 3:392–399
31. Pistone A, Sagnella A, Chieco C, Posati T, Varchi G, Formaggio F, Bertazza G, Saracino E, Caprini M, Bonetti S, Toffanin S, Divirgilio N, Muccini M, Rossi F, Ruani G, Zamboni R, Benfenati V (2016) Silk fibroin film from Golden-Yellow *Bombyx mori* is a biocomposite that contains lutein and promotes axonal growth of primary neurons. *Biopolymers* 105:287–299
32. Dionigi C, Posati T, Benfenati V, Sagnella A, Pistone A, Bonetti S, Ruani G, Dinelli F, Padeletti G, Zamboni R, Muccini M (2014) Nanostructured conductive bio-composite of silk fibroin/single walled carbon nano tube. *J Mater Chem B* 10:1424–1431
33. Terkaj W, Tolio T (2019) The italian flagship project: factories of the future. In: Tolio T, Copani G, Terkaj W (eds) *Factories of the future*. Springer

Open Access This book is licensed under the terms of the Creative Commons Attribution 4.0 International License (<http://creativecommons.org/licenses/by/4.0/>), which permits use, sharing, adaptation, distribution and reproduction in any medium or format, as long as you give appropriate credit to the original author(s) and the source, provide a link to the Creative Commons licence and indicate if changes were made.

The images or other third party material in this book are included in the book's Creative Commons licence, unless indicated otherwise in a credit line to the material. If material is not included in the book's Creative Commons licence and your intended use is not permitted by statutory regulation or exceeds the permitted use, you will need to obtain permission directly from the copyright holder.

